ELSEVIER

Magnetic Resonance Imaging 21 (2003) 593–598

MAGNETIC RESONANCE IMAGING

Improving spatiotemporal resolution of USPIO-enhanced dynamic imaging of rat kidneys

Ying Sun[a], Dewen Yang[b], Qing Ye[b], Mangay Williams[b], José M.F. Moura[a], Fernando Boada[c], Zhi-Pei Liang[d,*], Chien Ho[b]

[a]*Department of Electrical and Computer Engineering Carnegie Mellon University, Pittsburgh, PA, USA*
[b]*Pittsburgh NMR Center for Biomedical Research Department of Biological Sciences Carnegie Mellon University, Pittsburgh, PA, USA*
[c]*Department of Radiology University of Pittsburgh, Pittsburgh, PA, USA*
[d]*Department of Electrical and Computer Engineering University of Illinois at Urbana-Champaign, Urbana, IL, USA*

Received 14 June 2002; accepted 3 December 2002

Abstract

This paper addresses the problem of enhancing spatiotemporal resolution of ultra-small superparamagnetic iron oxide (USPIO)-enhanced dynamic MRI of rat kidneys. To alleviate the limited resolution problem of conventional full-scan Fourier imaging methods, we use a generalized series-based imaging scheme to reduce coverage of *k*-space. Experimental results demonstrate that the generalized series imaging method with basis functions constructed using two references (pre- and post-contrast) can reduce the number of phase encodings measured during the dynamic contrast wash-in process by a factor of 4 with a negligible or minimal loss of image quality. The method is expected to make 3D studies possible using USPIO-enhanced dynamic imaging of rat kidneys, and prove valuable for early detection of renal rejection after kidney transplantation.

1. Introduction

Kidney transplantation is widely used for treating patients with end-stage renal disease [1,2]. Because of the prevalence of graft failure, reliable noninvasive imaging techniques for early detection of renal rejection are extremely valuable. Scintigraphy has been used for evaluating functional abnormalities, whereas color Doppler ultrasonography and contrast-enhanced MRI often provide more anatomic details [3]. Color Doppler ultrasonography is useful for detecting segmental infarction or large areas of cortical necrosis [4] but is not sensitive enough for diagnosis of superficial cortical necrosis or small peripheral perfusion defects, particularly in the case of hemorrhagic necrosis [3]. Dynamic contrast-enhanced renal MRI can provide both morphologic and functional information with regard to excretory function, renal perfusion, and blood flow [5]. The most commonly used MR contrast agents are gadolinium chelates, which are filtered freely by the glomerulus without tubular secretion or reabsorption and have no known nephrotoxicity. However, using gadolinium chelates, the vascular and tubular phases are difficult to distinguish, especially at the end of the first pass, due to interstitial diffusion and elimination by glomerular filtration. Dextran-coated ultrasmall superparamagnetic iron oxide (USPIO) particles are known to have an intravascular distribution, migrate very slowly across the capillary endothelium, and have a relatively long blood half-life [6,7]. The slow elimination of these particles allows analysis of the blood pool tracer-related signal modifications, which remain stable during the observation period.

In our previous studies, USPIO-enhanced dynamic MRI experiments were carried out on normal and transplanted rat kidneys using a FLASH sequence with data acquisition parameters: $\alpha = 15°$, TE = 2.1 ms and TR = 3.45 ms. The temporal resolution (taking into account of the time delay due to duty cycle constraints) was about 334 ms [8]. This paper investigates the use of reduced-encoding imaging to improve the spatiotemporal resolution of USPIO-enhanced dynamic MRI.

Although reduced-encoding imaging traditionally results in a significant loss of image quality, recent methods based on the data-sharing principle are able to produce high-resolution dynamic images with as few as 16 encodings per

* Corresponding author. Tel.: +1-217-244-4023; fax: +1-217-244-0105.
E-mail address: z-liang@uiuc.edu (Z-P. Liang).

0730-725X/03/$ – see front matter
doi:10.1016/S0730-725X(03)00089-4

frame. A common feature of these methods is that a high-resolution reference image and a sequence of reduced dynamic data sets (usually in central *k*-space) are collected. Assuming that *N* encodings are collected for the reference data set and *M*encodings for each of the dynamic data sets, a factor of *N/M* improvement in temporal resolution (or imaging efficiency) is gained. In image reconstruction, the reference data are used to compensate for the loss of high frequency data in the dynamic data sets. In the keyhole method [9,10], this is done in a straightforward fashion, that is, the unmeasured encodings of each dynamic data set are replaced directly by the corresponding reference data to create a "full-size" data set. A weakness of this data-sharing method is that any data inconsistency between the dynamic and reference data sets will result in data truncation artifacts and, as a result, dynamic image features are produced only at low resolution. With RIGR (Reduced-encoding Imaging by Generalized-series Reconstruction), image reconstruction is done using a generalized series model [11,12], in which the basis functions are determined by the reference data and the coefficients are determined by the dynamic data. This reconstruction algorithm is approximately optimal in the minimum cross-entropy sense [11] and can overcome the limited resolution problem with the keyhole method. It has also been shown that with multiple references, RIGR can reconstruct dynamic features in a resolution close to that of the reference image [13,14]. In this paper, we will use an improved algorithm based on two references to construct a set of basis functions for fast imaging of the wash-in/wash-out process of USPIO particles in rat kidneys.

The rest of the paper is organized as follows: Section 2 describes the proposed method in detail; Section 3 presents some simulation and experimental results; and Section 4 concludes the paper.

2. Proposed method

The proposed method is based on a generalized series (GS) imaging scheme in which an unknown image function is expressed as [11]

$$I(\vec{x}) = \sum_n c_n \varphi_n(\vec{x}). \tag{1}$$

The basis functions $\varphi_n(\vec{x})$ are given by

$$\varphi_n(\vec{x}) = w(\vec{x}) e^{i2\pi n \Delta \vec{k} \vec{x}}, \tag{2}$$

where the weighting function $w(\vec{x})$ is chosen based on a priori information. Treating $w(\vec{x})$ as an initial estimate of $I(\vec{x})$, the basis functions in Eq. (2) are approximately optimal according to the minimum cross-entropy principle [11]. After $w(\vec{x})$ is determined, the series coefficients can be found by solving a set of simultaneous linear equations [11]. We next describe how to use this model to improve spatio-temporal resolution of USPIO-enhanced dynamic imaging of rat kidneys.

2.1. Data acquisition

The data acquisition scheme of the proposed method is similar to that of the two-reference RIGR method (TRIGR) [13,14], which is characterized by: (a) the acquisition of two high-resolution reference images, one pre-contrast image as the baseline reference and another after the rapid dynamic wash-in phase is completed; and (b) acquisition of a sequence of reduced data sets during the dynamic process. The number of encodings collected for the references is determined in principle by the desired spatial resolution whereas the number of encodings for the dynamic data sets is set based on the desired temporal resolution. In our preliminary 2D imaging experiments, 64 phase encodings were collected for the reference data sets and 16 for the dynamic data sets in the center of *k*-space, and a FLASH sequence was used for signal generation in which $\alpha = 15°$, TE = 2.1 ms an TR = 3.45 ms. The experiments were performed on Brown Norwegian rats with USPIO dose of 12.1 mg Fe/kg body weight. The MR data acquisition was done in a 4.7-T, 40-cm horizontal bore Bruker AVANCE DRX MR instrument using a 7-cm diameter Bruker volume transceiver RF coil. Further details on the experimental protocol can be found in [8].

2.2 Image reconstruction

Let $I_{r,1}(\vec{x})$ and $I_{r,2}(\vec{x})$ be the high-resolution reference images, and $d_q(\vec{k})$, $1 \le q \le Q$, be dynamic data sets such that

$$d_q(\vec{k}) = \int I_q(\vec{x}) e^{-i2\pi \vec{k}\vec{x}} \, d\vec{x}, \tag{3}$$

where $I_q(\vec{x})$ are the desired dynamic images. In USPIO-enhanced dynamic MRI, $I_{r,1}(\vec{x})$ can be treated as the baseline such that $I_{r,2}(\vec{x}) - I_{r,1}(\vec{x})$ highlights areas of dynamic signal variations. Consequently, we set

$$w(\vec{x}) = |I_{r,2}(\vec{x}) - I_{r,1}(\vec{x})|, \tag{4}$$

and

$$\Delta d_q(\vec{k}) = d_q(\vec{k}) - d_{r,1}(\vec{k}), \tag{5}$$

where $d_{r,1}(\vec{k})$ is the pre-contrast reference data and $\Delta d_q(\vec{k})$ is calculated at the *k*-space locations in which $d_q(\vec{k})$ is available. Let $\Delta I_q(\vec{x})$ represent the dynamic signal changes between the *q*th data set and the pre-contrast reference image $I_{r,1}(\vec{x})$, $I_q(\vec{x})$ can be expressed as

$$I_q(\vec{x}) = I_{r,1}(\vec{x}) + \Delta I_q(\vec{x}). \tag{6}$$

The question now is how to reconstruct $\Delta I_q(\vec{x})$ in high resolution. This can be done by applying the GS model

directly to $\Delta d_q(\vec{k})$ using the basis functions constructed based on the weighting function given in Eq. (4). An FFT-based fast algorithm is also available to reconstruct $\Delta I_q(\vec{x})$. More specifically, we first rewrite the GS model in the following form:

$$\Delta I_q(\vec{x}) = w(\vec{x})C(\vec{x}), \tag{7}$$

where $C(\vec{x}) = \sum_n c_n e^{-i2\pi\vec{k}_n} \cdot \vec{x}$ is the contrast modulation function. Let $\Delta\hat{I}_q(\vec{x}) = I_q(\vec{x}) * h(\vec{x})$ be the low-resolution Fourier reconstruction of $\Delta I_q(\vec{x})$ from the measured k-space data, where $h(\vec{x})$ is the point spread function of the data truncation window. We then have

$$\Delta\hat{I}_q(\vec{x}) = [w(\vec{x})C(\vec{x})]*h(\vec{x}). \tag{8}$$

Noting that $C(\vec{x})$ is a smooth function [in the sense that $C(\vec{x})$ does not vary significantly over any region of the shape and size of the effective spatial support of $h(\vec{x})$], we can factor $C(\vec{x})$ out of the convolution integral in Eq. (8). Consequently, we have

$$\Delta\hat{I}_q(\vec{x}) \approx [w(\vec{x}) * h(\vec{x})]C(\vec{x}) = \hat{w}(\vec{x})C(\vec{x}) \tag{9}$$

where $\hat{w}(\vec{x}) = w(\vec{x}) * h(\vec{x})$ is a low-resolution version of $w(\vec{x})$, which is obtained by discarding the high spatial frequency data that produced $w(\vec{x})$. From Eq. (9), we immediately obtain

$$C(\vec{x}) = \frac{\Delta\hat{I}_q(\vec{x})}{\hat{w}(\vec{x})}. \tag{10}$$

The above equation provides a fast way to evaluate $C(\vec{x})$ because the main computation here is the two FFTs used to calculate $\Delta\hat{I}_q(\vec{x})$ and $\hat{w}(\vec{x})$. The solution provided by Eq. (10) could be unstable due to division by zero (or numbers close to zero). The problem can be easily dealt with by adding a "regularization" constant λ to the magnitude of $\hat{w}(\vec{x})$ such that

$$C(\vec{x}) = \frac{\Delta\hat{I}_q(\vec{x})}{[|\hat{w}(\vec{x})| + \lambda]e^{i\theta(\vec{x})}}, \tag{11}$$

where $\theta(\vec{x})$ is the phase function of $\hat{w}(\vec{x})$. Clearly, a large λ will give a more stable $C(\vec{x})$, but at the expense of accuracy. We set $\lambda = 10^{-2}\,\mu$, with μ being the mean value of $|\hat{w}(\vec{x})|$, which gave acceptable results.

3. Results and discussion

We present in this section some representative simulation and experimental results to illustrate the performance of the proposed method.

Fig. 1 shows a set of simulation results based on the experimental data acquired from a USPIO-enhanced dynamic imaging experiment. In this experiment, we acquired, as the "gold" standard, a sequence of 64 dynamic images with "high" spatial resolution (64 × 64 phase encodings were used to avoid excessive temporal averaging). We then truncated the measured k-space data in both directions to obtain a reduced data set with 16 ×16 phase encodings for each data frame. Such data frames could be obtained using a single-shot spiral or EPI sequence [15]. In image reconstruction, two methods were used: the conventional Fourier method and the proposed TRIGR method (using the FFT-based reconstruction algorithm described in Section 2.2). The reconstruction results for 12 temporal frames are presented in Fig. 1 along with the "gold" standard images (Fig. 1a). As can be seen from Fig. 1b, the images reconstructed using the Fourier transform contain significant blurring artifacts and, as a result, it is very difficult to distinguish the anatomic structures in these images. In contrast, the images reconstructed using the proposed method (shown in Fig. 1c) have a much better spatial resolution, comparable to that of the "gold" standard in Fig. 1a. Anatomic structures, particularly the boundaries of the two kidneys are "equally" well defined in both the TRIGR images and the "gold" standard while TRIGR uses only 1/16 of the data for each data frame, providing potentially a factor of 16 improvement in temporal resolution for 3D imaging experiments.

To illustrate the performance of the proposed method in the practical setting of USPIO-enhanced dynamic imaging of rat kidneys, we directly implemented the TRIGR imaging scheme by collecting reduced dynamic data sets to gain temporal resolution. As this was a 2D study, we collected for each data frame 16 phase encodings, each with 64 data points along the readout direction. Fig. 2 shows the results of this experiment where (a) displays the two reference images with 64 phase encodings: pre-contrast (left) and post-contrast (right); (b) shows 12 out of the 128 image frames reconstructed using the conventional Fourier method; and (c) shows the corresponding images reconstructed using TRIGR with basis functions constructed using the references in (a). As expected, the Fourier images in Fig. 2b contain serious blurring artifacts, rendering the images useless for practical use. The blurring is essentially removed by TRIGR in Fig. 2c. An important practical question here is: would TRIGR, in applying the constraints to the dynamic images, bias the temporal response of different tissues to the injected USPIO? To address this question, we calculated the temporal response curves based on the TRIGR and Fourier images reconstructed from the experimental data. A set of representative results is shown in Fig. 3a that contains the temporal responses in two important areas: cortex (black) and muscle (gray), for the sequences reconstructed with conventional Fourier method (circle) and the proposed TRIGR method (star), respectively. In this study we selected the spatial locations carefully (labeled with letter "A" and "B" in Fig. 3b) so that the partial-volume (or spatial averaging) effect in the Fourier images (due to low spatial resolution) does not affect the temporal response significantly at these locations. As can be seen in Fig. 3a, TRIGR reproduced the temporal responses very well. In other words, TRIGR did not introduce any noticeable bias to the temporal behavior of contrast uptake in these tissues while

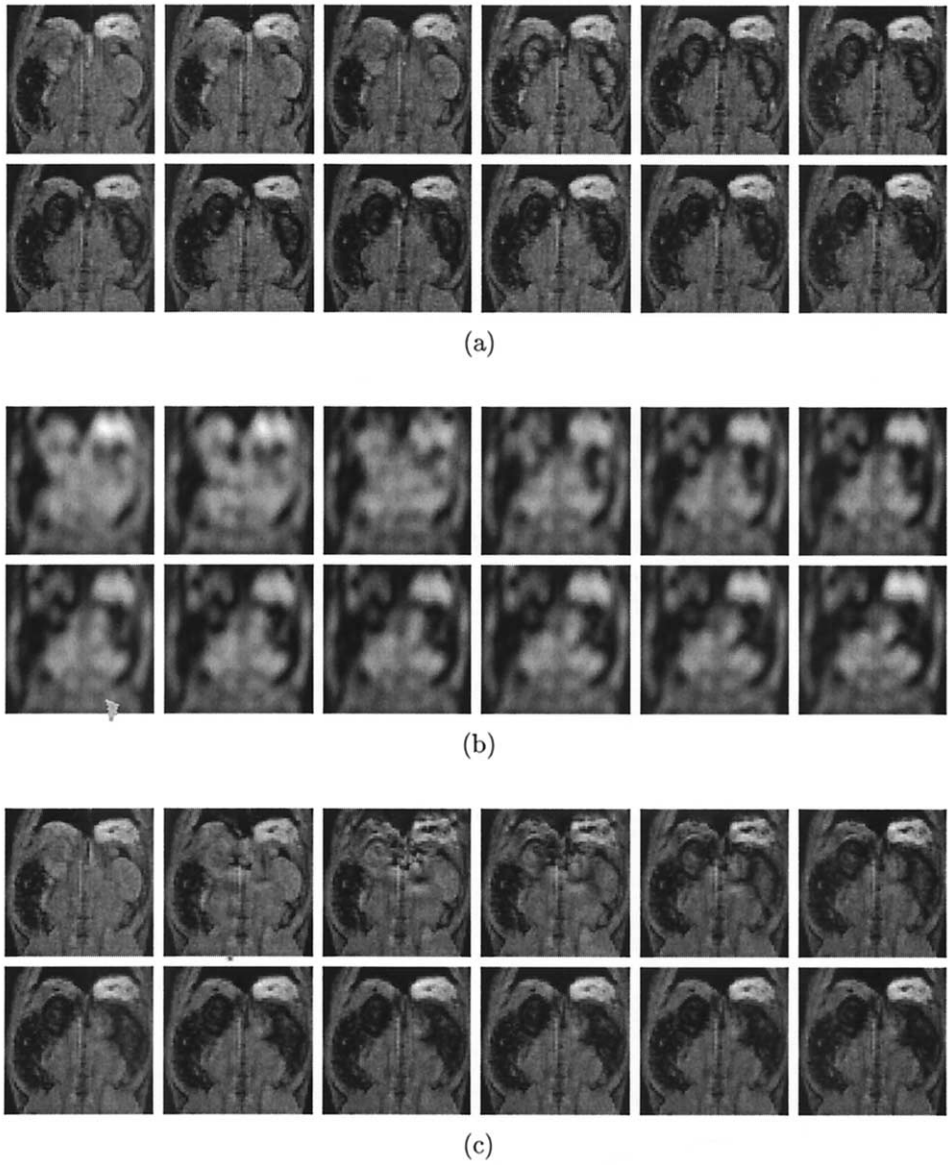

Fig. 1. Dynamic images of a rat kidney reconstructed using: (a) the conventional Fourier method with 64 × 64 data points ("gold" standard), (b) the conventional Fourier method with 16 × 16 central *k*-space points, and (c) the proposed method with the same data in (b). Notice the significant resolution loss in (b), which is removed by the proposed method.

dramatically improving the spatial resolution of the Fourier images. This is a very desirable property, which indicates that USPIO-enhanced dynamic imaging of rat kidneys with good spatiotemporal resolution can be achieved by data sharing using the proposed imaging scheme.

4. Conclusion

Kidney transplantation is widely used as the treatment of choice for patients with end-stage renal disease. Because of the prevalence of graft failure, reliable noninvasive imaging techniques for early detection of renal rejection are extremely valuable. This paper is concerned with the development of a fast method for USPIO-enhanced dynamic imaging of rat kidneys. To alleviate the limited resolution problem of conventional full-scan Fourier imaging methods, we use a generalized series-based imaging scheme to reduce coverage of the *k*-space. Experimental results demonstrate that the proposed method with basis functions constructed using two references (pre- and post-contrast) coupled with appropriate pulse sequences can reduce the number of phase encodings by a factor of up to 4 in 2D studies. It is expected to provide a reduction factor of up to 16 in 3D imaging studies. We can take advantage of these properties to significantly speed-up the imaging process, which should prove very valuable for early detection of renal rejection after kidney transplantation.

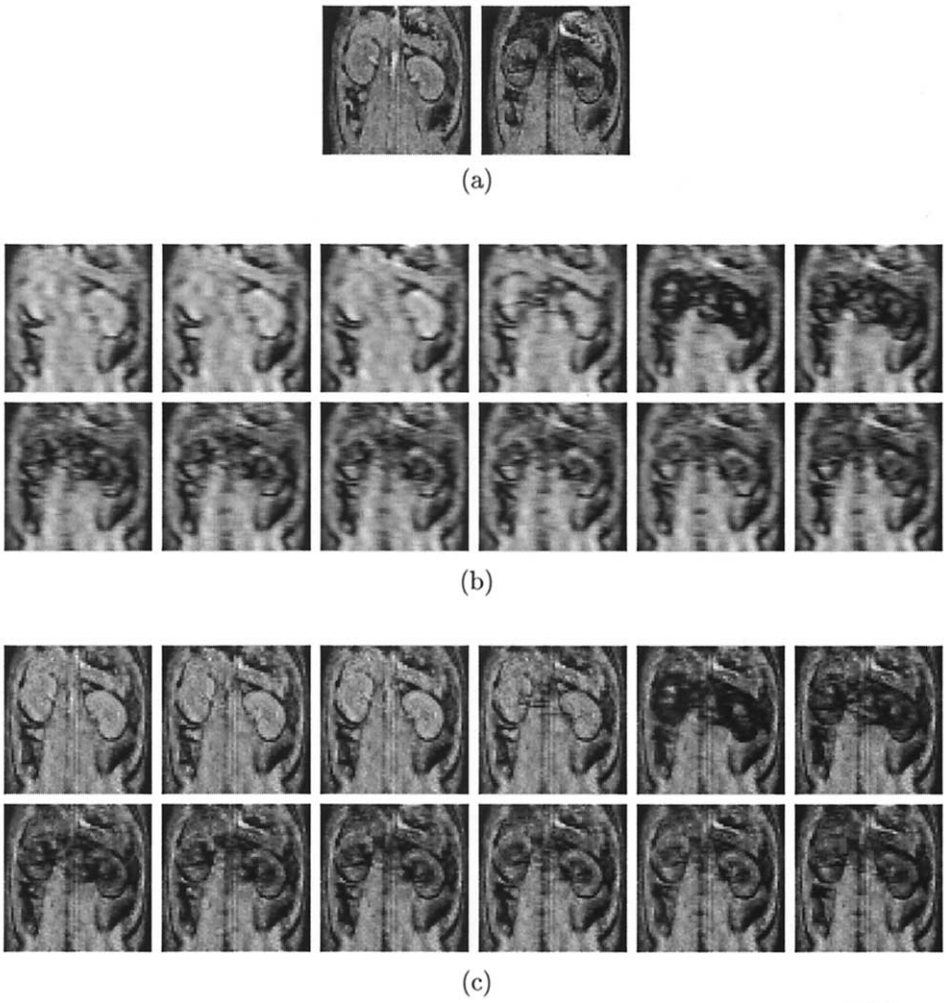

Fig. 2. Sectional images of a rat kidney obtained in a USPIO-enhanced imaging study: (a) high-resolution pre- and post-contrast images obtained with 64 encodings; (b) dynamic images during the wash-in/wash-out period obtained using the conventional Fourier method with 16 phase encodings, and (c) dynamic images obtained using the proposed method with 16 phase encodings and basis functions constructed based on the references in (a).

Acknowledgments

The work reported in this paper was supported in part by: NIH-R21-HL62336-01, NIH-R01-HL-64205-01, NIH-P41RR-03631, NIH-R01RR/AI-15187, and the UIUC University Scholar Award.

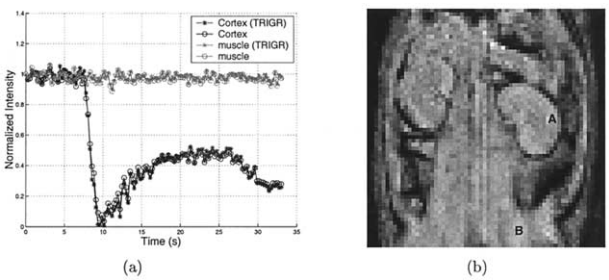

Fig. 3. (a) Temporal responses calculated from image sequences in Figs. 2 (b)-(c) at the spatial locations marked in gray-scale image in (b).

References

[1] US. Department of Health and Human Services. Annual report of the U.S. scientific registry of transplant recipients and the organ procurement and transplantation network: transplant data: 1990-1999. Public Health Service, Bureau of Health Resources Department, Division of Organ Transplantation, Bethesda, MD; UNOS, Richmond, VA; 2000.

[2] Rigg KM. Renal transplantation: current status, complications and prevention. J Antimicrob Chemother 1995;36(Suppl):B51–7.

[3] Helenon O, Attlan E, Legendre C, Hanna S, Denys A, Souissi A, Kreis H. Gd-DOTA-enhanced MR imaging and color Doppler US of renal allograft necrosis. Radiographics 1992;12:21–33.

[4] Grenier N, Douws C, Morel D, Ferriere JM, Le Guillou M, Potaux L, Broussin J. Detection of vascular complications in renal allografts with color Doppler flow imaging. Radiology 1991;178:217–23.

[5] Krestin GP. Magnetic resonance imaging of the kidneys: current status. Magn Reson Q 1994;10:2–21.

[6] Trillaud H, Degreze P, Combe C, Palussiere J, Chambon C, Grenier N. Evaluation of intrarenal distribution of ultrasmall superparamagnetic iron oxide particles by magnetic resonance imaging and modification by furosemide and water restriction. Invest Ratiol 1994;29: 540–6.

[7] Weissleder R, Elizondo G, Wittenberg J, Rabito CA, Bengele HH, Josephson L. Ultrasmall superparamagnetic iron oxide: characterization of a new class of contrast agents for MR imaging. Radiology 1990;175:489–93.
[8] Yang D, Ye Q, Williams M, Sun Y, Hu TCC, Williams DS, Moura JMF, Ho C. USPIO-enhanced dynamic MRI: evaluation of normal and transplanted rat kidneys. Magn Reson Med 2001;46:1152–63.
[9] van Vaals JJ, Tuithof HH, Dixon WT. Increased time resolution in dynamic imaging. Proc. SMRI, 10th Annual Meeting. 1992: p. 44.
[10] Brummer ME, Dixon WT, Gerety B, Tuithof H. Composite k-space windows (keyhole techniques) to improve temporal resolution in a dynamic series of images following contrast administration. In: Book of abstracts: Eleventh Annual Meeting of the Society of Magnetic Resonance in Medicine. Berkeley, CA: SMRM; 1992: p. 4236.
[11] Liang ZP, Lauterbur PC. An efficient method for dynamic magnetic resonance imaging. IEEE Trans Med Imaging 1994;13:677–86.
[12] Liang ZP, Ji X, Hess C. Motion-compensated keyhole/rigr imaging. Proc. 8th Ann. Meeting ISMRM. Denver, CO: ISMRM; 2000: p. 1697.
[13] Hanson JM, Liang ZP, Wiener EC, Lauterbur PC. Fast dynamic imaging using two reference images. Magn Reson Med 1996;36: 172–5.
[14] Liang ZP. Generalized series dynamic imaging. Proc. Int. Workshop Med. Imaging and Augmented Reality. Hong Kong: MIAR; 2001.
[15] Schmitt F, Stehling MK, Turner R. Echo-Planar Imaging: Theory, Technique, and Application. Berlin: Springer-Verlag, 1998.